Hindawi
International Journal of Antennas and Propagation
Volume 2022, Article ID 3447055, 9 pages
https://doi.org/10.1155/2022/3447055

Research Article

Design and Analysis of a Metamaterial-Inspired Miniaturized Quadband Antenna

Si Li, Shitao Sun, and Yunlong Mao

School of Electronics and Information, Jiangsu University of Science and Technology, Zhenjiang, Jiangsu, China

Correspondence should be addressed to Si Li; lisi0511@just.edu.cn and Yunlong Mao; maoyunlong0511@just.edu.cn

Received 12 January 2022; Revised 14 February 2022; Accepted 22 February 2022; Published 27 March 2022

Academic Editor: Shah Nawaz Burokur

A metamaterial-inspired miniaturized quadband antenna is designed and discussed with a transmission line model to study the theory of miniaturization and multiband in this paper. A conventional printed monopole antenna is assumed as a primary antenna and then surrounded by an array of 4 × 2 interdigital LHMs. The proposed antenna has a compact size of 36mm × 24mm × 1mm, and operates at 2.40–2.55 GHz, 3.02–3.38 GHz, 5.04–5.52 GHz, and 7.08–7.38 GHz. Good gain and omnidirectional radiation patterns are observed in simulations and measurements. A simplified transmission line modal was established to study the reasons for miniaturization and multiband that were brought about by the LHM array. Related results verified the theoretical analysis and indicated that the proposed antenna is a good candidate for wireless communication applications.

1. Introduction

In modern wireless systems, a common trend for antennas is to be miniaturized while maintaining good radiation properties to fulfill multiband requirements, especially for ongoing wireless communication systems.

Various types of miniaturized multiband antennas were reported. In some of these designs, multiband property is archived with different shaped strips, such as the C- and L-shapes [1], the Y-shape [2], and the rhombus shape [3]. In some other designs, multiband property is archived by etching different slots, such as the U-shape [4, 5], the F-shape [6], and the T-shape [7] slots. Recently, metamaterials have been investigated for antenna miniaturization and enabling multiband operation [8]. Different kinds of split-ring resonators (SRRs) are used in antenna designs [9–15]. Among these designs, SRRs were used as radiating elements [10–12] to surround the radiating elements [13], or were printed on the ground plane side of the radiating elements [9, 14, 15]. Especially, in [11, 13, 14], the special personality of the metamaterials is designed to generate required passing bands of the proposed antennas, while in [12], it is responsible for the notched bands. In some other designs, metamaterials are used as near-field resonant parasitic (NFRP) elements [16–19], for the purpose to increase effective inductance and capacitance, hence achieving miniaturization and multiband. However, it would be better if a transmission model could be established to analyze the mechanism for miniaturization and multiband properties in detail.

In this work, a metamaterial-inspired miniaturized quadband antenna is presented. The proposed antenna has a compact size of 36mm × 24mm × 1mm ($0.27\lambda \times 0.18\lambda \times 0.008\lambda$) and is printed on an FR4 substrate with a tangent loss of 0.02. A conventional printed monopole is assumed as the primary antenna. Later, a 4 × 2 array of interdigital LHM is applied to surround the monopole. This LHM is verified with negative permeability and permittivity from 2.75 GHz to 3.75 GHz. The proposed antenna works at 2.40–2.55 GHz, 3.02–3.38 GHz, 5.04–5.52 GHz, and 7.08–7.38 GHz. Compared to the conventional monopole, the employment of LHMs not only reduced antenna size, but also added two more frequency bands. A simplified transmission line model for the proposed antenna has been established, and the mechanism of LHMs as NFRP

elements is analyzed. The proposed antenna is fabricated and measured, and the results match well with simulations. Finally, a conclusion is drawn, pointing out that the proposed antenna is a good candidate for wireless communication applications.

2. Antenna Design Procedure

2.1. Left-Handed Metamaterial Design. For the purpose of multiresonances and miniaturization, an interdigital LHM is designed as shown in Figure 1. This structure is printed on an FR4 substrate with relative permeability equals to 4.4 and its thickness is 1 mm. The parameters are listed in Table 1.

This LHM unit is composed of a few coupled strips, providing magnetic resonance; the currents are forced to flow in a vertical direction, providing electric resonance. Therefore, this LHM should be capable of exhibiting double negative properties.

Simulations were operated and the results are displayed in Figure 2. It is observed that there are two resonances, and the passing band is from 2.0 GHz to 3.27 GHz. Therefore, this LHM is capable of generating resonances at frequencies of around 2.4 GHz.

To investigate its electromagnetic properties, we apply 'S parameter Retrieval' method [20]. Retrieved effective permeability, permittivity, impedance, and refractive index are displayed in Figure 3.

Figure 3(a) displayed the retrieved effective permittivity, as observed, was negative at the frequency from 2.75 GHz to 4 GHz. Figure 3(b) displayed the retrieved effective permeability, which is negative at the frequency range from 2.75 GHz to 3.45 GHz. Therefore, the proposed LHM exhibits double negative property and negative refractive index (Figure 3(d)) at the frequency range from 2.75 GHz to 3.45 GHz.

2.2. Design of the LHM-Inspired Antenna. The design procedure of this antenna is shown in Figure 4.

First, a conventional monopole antenna (Ant 1) is designed. A rectangular slot is etched on the ground for the purpose of impedance matching. This monopole works at two different frequency ranges, which correspond to the first and third resonances, respectively. Later, 4 LHM elements are applied to surround the monopole. For further miniaturization and better impedance matching, another four LHM elements are added. The parameters for this antenna are listed in Table 2.

Simulations were operated for all 3 antennas. The proposed antenna (Ant 3) is also fabricated and measured, as displayed in Figure 5. Simulated and measured S parameters are displayed in Figure 6, and their corresponding working bands are listed in Table 3.

Compared to the primary monopole antenna, the introduction of LHMs has brought significant miniaturization as the first working frequency has been shifted from 2.7 GHz (Ant 1) to 2.4 GHz (Ant 3). Additionally, two more working frequencies are observed, achieving multiband property.

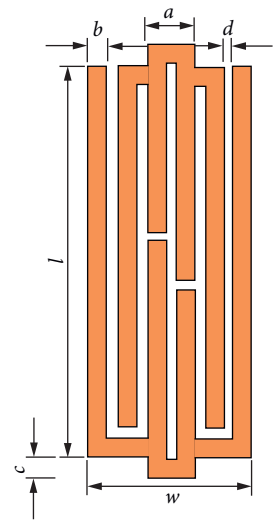

Figure 1: Structure of the designed LHM unit.

The radiating pattern of the proposed antenna is also simulated and measured at 4 different resonances, as displayed in Figure 7. Good agreements are also obtained. Gain and radiation efficiency are also obtained through simulation, as displayed in Figure 8. The efficiency is greater than 46% and as high as 93%. Even at a few frequencies, the gain is smaller than 0 dBi. However, at higher frequencies, the peak gain can be as large as 3.8 dBi. Therefore, the proposed antenna exhibits good gain and efficiency.

3. Analysis and Discussions of the proposed antenna

3.1. Transmission Line Model Analysis. To analyze its working principle, we start with the transmission line model. A conventional monopole antenna can be regarded as a transmission line, as illustrated in Figure 9, where L_0 and C_0 are the equivalent inductance and capacitance. Employment of LHMs is like adding an inductor and a capacitor to the transmission line model, as illustrated in Figure 10.

Strong near-field resonant coupling occurs between the monopole antenna and the LHMs. The simplified equivalent circuit is displayed in Figure 10, where C_1 and L_1 are mainly decided by LHMs. For a microsection in z direction Δz , one can obtain

$$\begin{cases} -\dfrac{\partial U}{\partial z} = (R_0 + j\omega L_0)I = Z_0 I, \\ -\dfrac{\partial I}{\partial z} = \left[G_0 + \dfrac{j\omega C_2}{1 - \omega^2 L_1 C_2} + j\omega C_1\right]U = Y_0 U, \end{cases} \tag{1}$$

where R_0 and G_0 are the corresponding impedance and conductance, Δt is a time sampling period.

Therefore, the character impedance is calculated as

Table 1: Parameters for an interdigital LHM unit.

l (mm)	w	a	b	c	d
10.5	4.5 mm	1.2 mm	0.5 mm	0.5 mm	0.2 mm

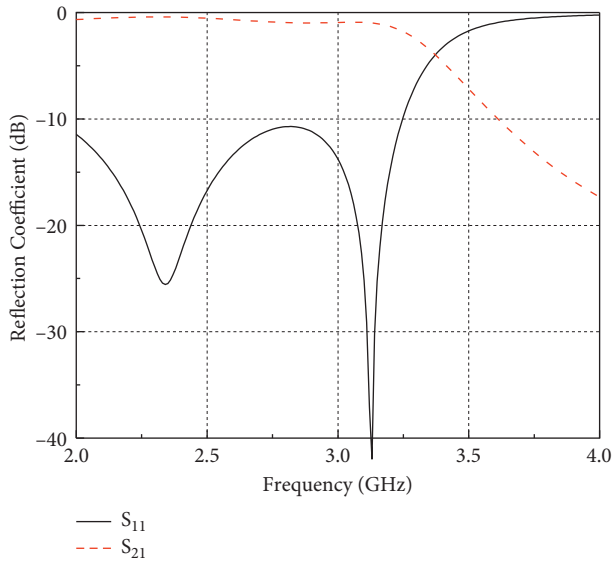

Figure 2: Simulated S parameters of the proposed LHM unit.

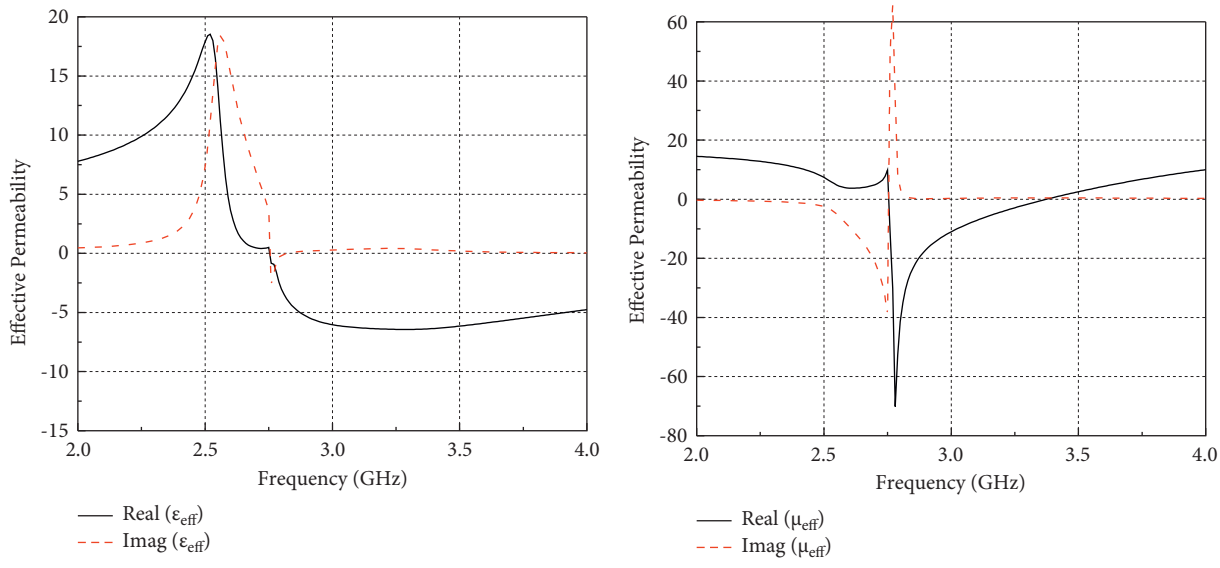

Figure 3: Continued.

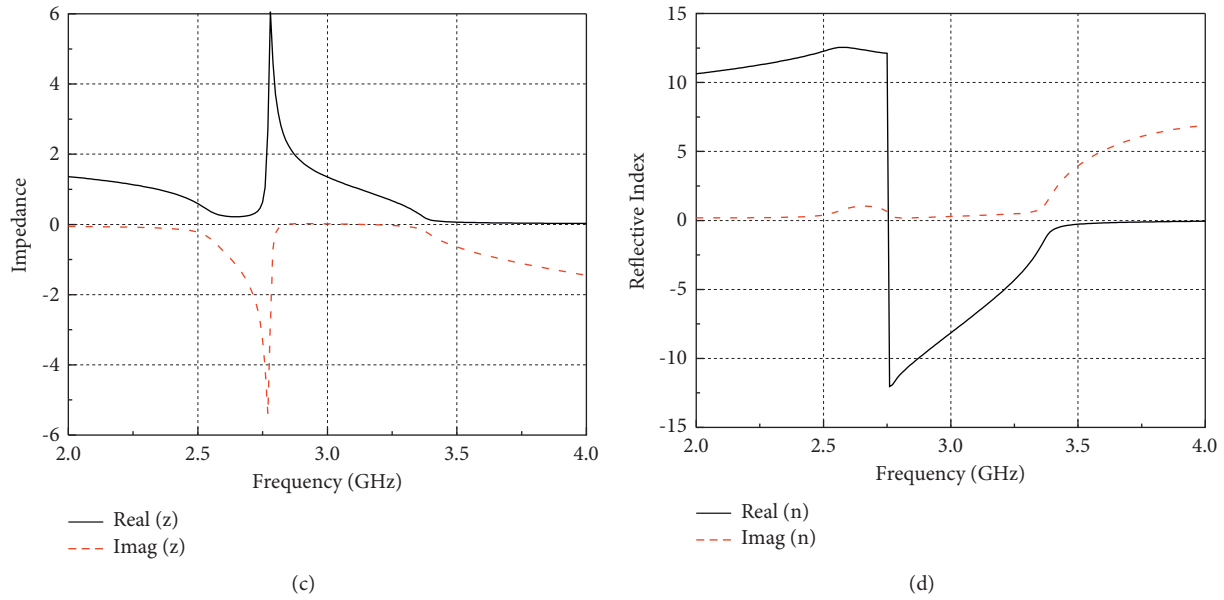

Figure 3: Retrieved effective parameters using 'S Parameters Retrieval Method:' (a) effective permittivity, (b) effective permeability, (c) normalized impedance, and (d) refractive index.

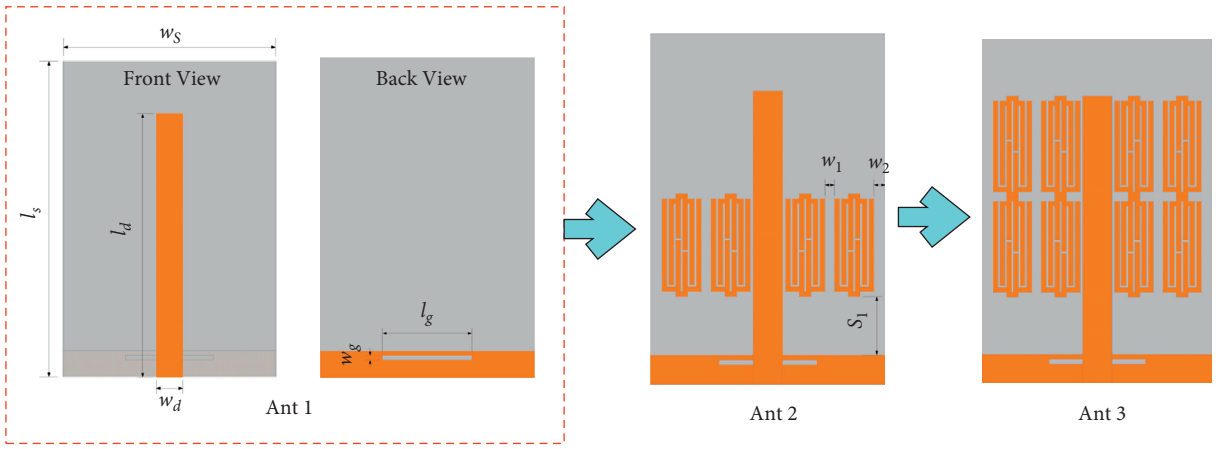

Figure 4: Design procedure of the proposed antenna.

Table 2: Parameters for the proposed antenna.

l_s (mm)	w_s	l_d	w_d	l_g	w_g
36	24 mm	30 mm	3 mm	10 mm	0.5 mm

$$Z_c = \sqrt{\frac{Z_0}{Y_0}} = \sqrt{\frac{R_0 + j\omega L_0}{G_0 + \left(j\omega C_2/1 - \omega^2 L_1 C_2\right) + j\omega C_1}} \approx \sqrt{\frac{L_0}{C_1 + \left(C_2/1 - \omega^2 L_1 C_2\right)}}. \quad (2)$$

And the input impedance can be expressed as

$$Z_{\text{in}}(l) = Z_c \frac{Z_L + jZ_c \tan \beta l}{Z_c + jZ_L \tan \beta l}. \quad (3)$$

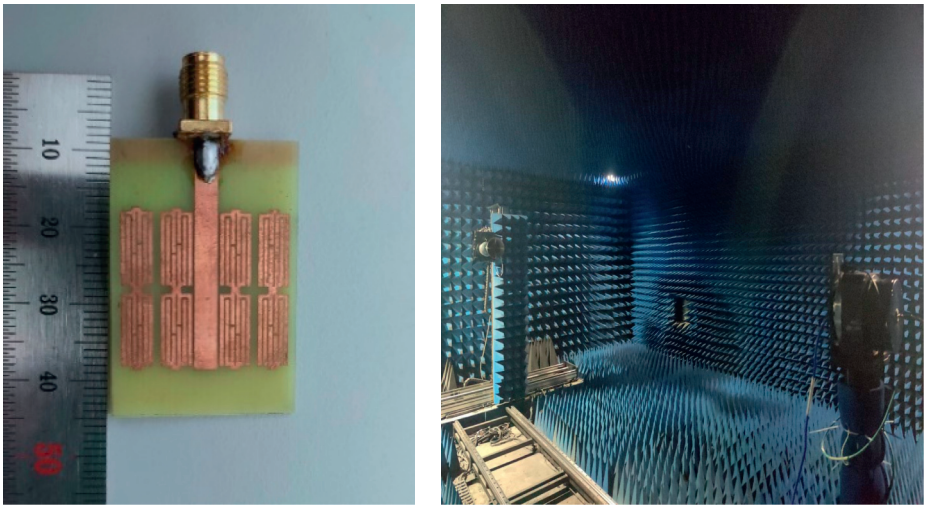

(a) (b)

Figure 5: Prototype of the proposed antenna and the measurement environment: (a) prototype of the proposed antenna and (b) measurement environment.

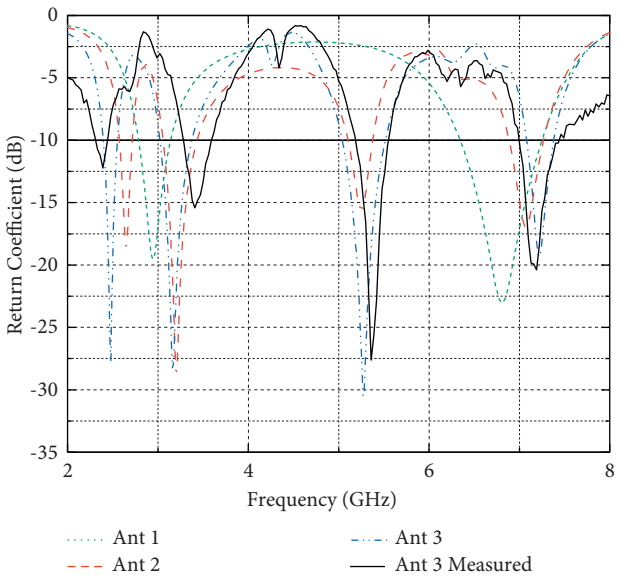

Figure 6: Simulated and measured S parameters.

Table 3: Working frequency ranges of different antennas.

Antenna	Frequency ranges (GHz) ($S_{11} < -10$ dB)			
Ant 1	2.7–3.07		6.17–7.04	
Ant 2	2.57–2.72	3.06–3.43	5.10–5.38	6.89–7.27
Ant 3	2.40–2.55	3.02–3.38	5.04–5.52	7.08–7.38
Ant 3 measured	2.30–2.46	3.28–3.59	5.18–5.56	6.98–7.44

At resonances, the imaginary part of the input impedance should be zero. Hence, we rewrite (3) as

$$Z_{\text{in}}(l) = Z_c \frac{1 + \tan^2(\beta l)}{Z_c^2 + Z_L^2 \tan^2(\beta l)} + jZ_c \frac{\left(Z_c^2 - Z_L^2\right)\tan(\beta l)}{Z_c^2 + Z_L^2 \tan^2(\beta l)}. \quad (4)$$

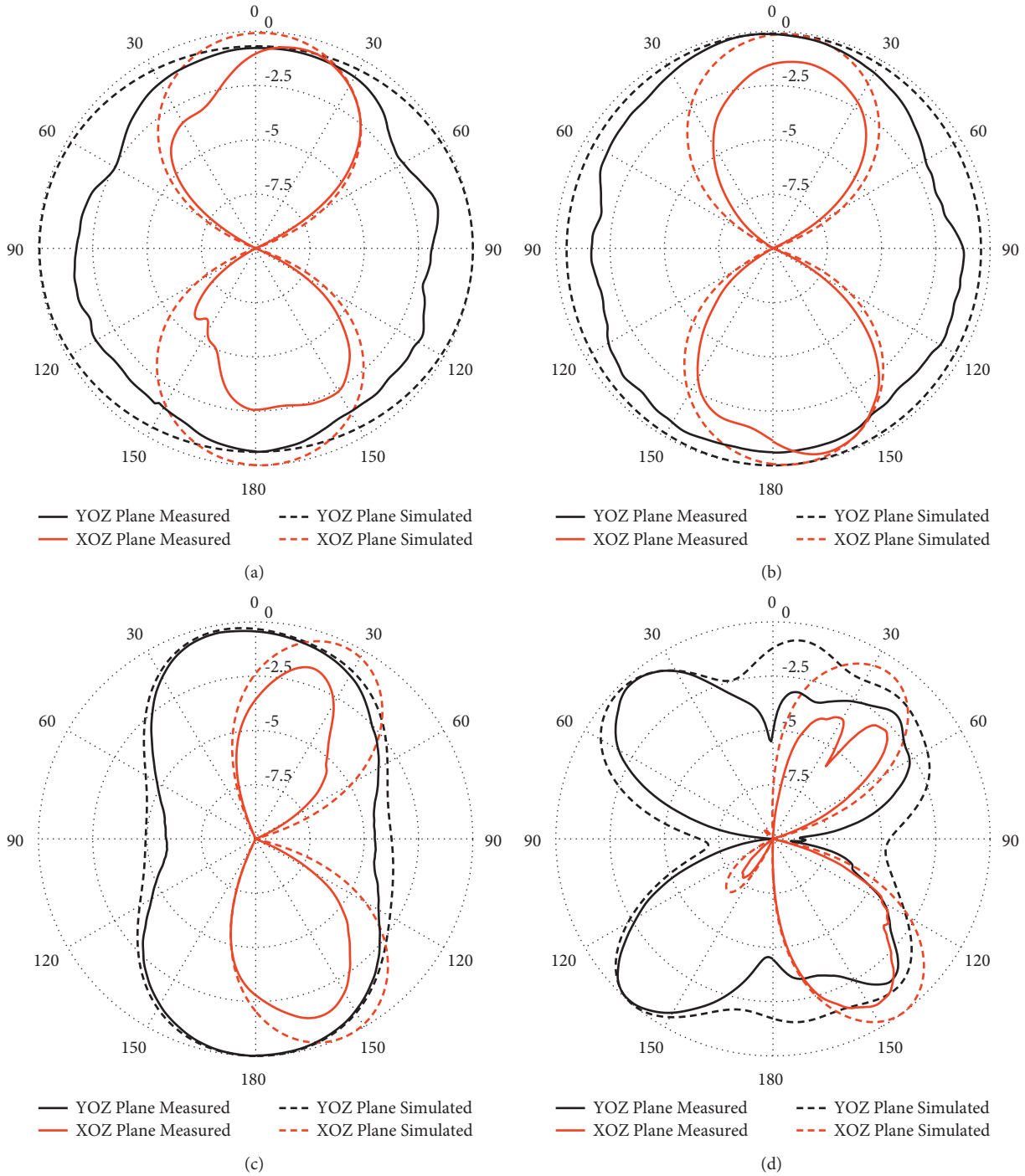

Figure 7: Radiation pattern of the proposed antenna at different resonances: (a) 2.49 GHz, (b) 3.22 GHz, (c) 5.23 GHz, and (d) 7.15 GHz.

That is to make

$$\left(Z_c^2 - Z_L^2\right)\tan(\beta l) = 0, \tag{5}$$

where $Z_L = (1/j\omega C_0)$.

From equation (5), if $\tan(\beta l) = 0$, since it is a period function, there will be higher harmonics that may bring more than one working band. On the other hand, if $Z_c^2 - Z_L^2 = 0$, we substitute (2) into equation (5), after a series of transformations, one can obtain that

$$\omega = \sqrt{\frac{L_0C_0 - L_1C_1C_2 \pm \sqrt{\left(L_1C_1C_2 + L_0C_0\right)^2 + 4L_1L_0C_0C_2^2}}{2L_1L_0C_0C_2}}. \tag{6}$$

That is to say, strong coupling between the monopole antenna and the LHMs will add working frequency ranges. Similarly, without LHM, the phase constant β is

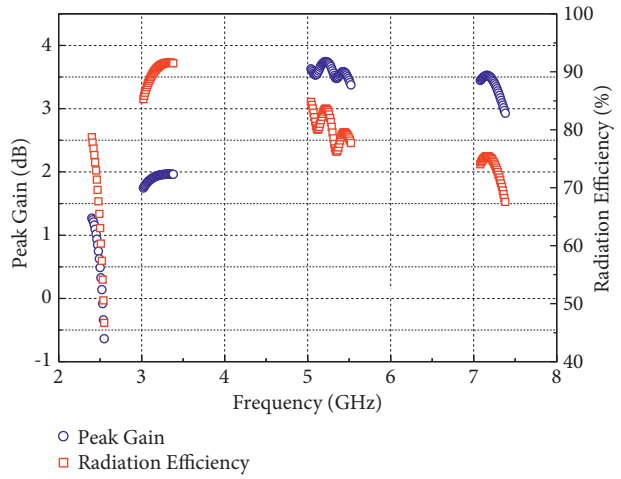

Figure 8: Gain and efficiency of the proposed antenna.

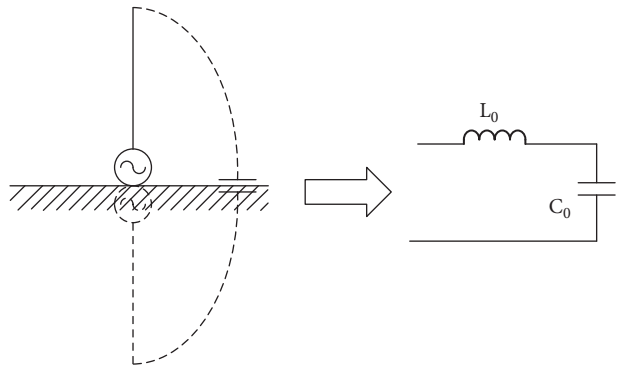

Figure 9: Equivalent circuit of conventional monopole antenna.

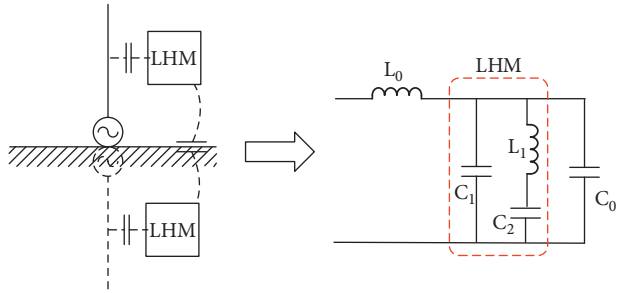

Figure 10: Equivalent circuit of conventional monopole with LHM.

$$\beta = \sqrt{\frac{1}{2}\left[\left(\omega^2 L_0 C_0 - R_0 G_0\right) + \sqrt{\left(R_0^2 + \omega_0^2 L_0^2\right)\left(G_0^2 + \omega_0^2 C_0^2\right)}\right]}. \tag{7}$$

However, the employment of LHMs will increase the conductance. We substitute $G_0 = G_0 + (j\omega C_2/1 - \omega^2 L_1 C_2)$ into (7), we figure out that larger G_0 will bring larger β, hence shorter l can make $\tan \beta l = 0$, thus achieving miniaturization.

3.2. Surface Current Distribution Analysis. Current distributions at 4 different resonances of the proposed antenna are also displayed in Figure 11. At these frequencies, strong coupled currents are observed flowing on the LHMs. However, since the LHM unit is symmetrical, the radiating far-field of these currents will cancel each other out, so they do not contribute to the far-field radiation. Thus, together with the transmission line model analysis, it is obvious that the LHMs only help to achieve miniaturization and multiband but will not affect far-field radiation.

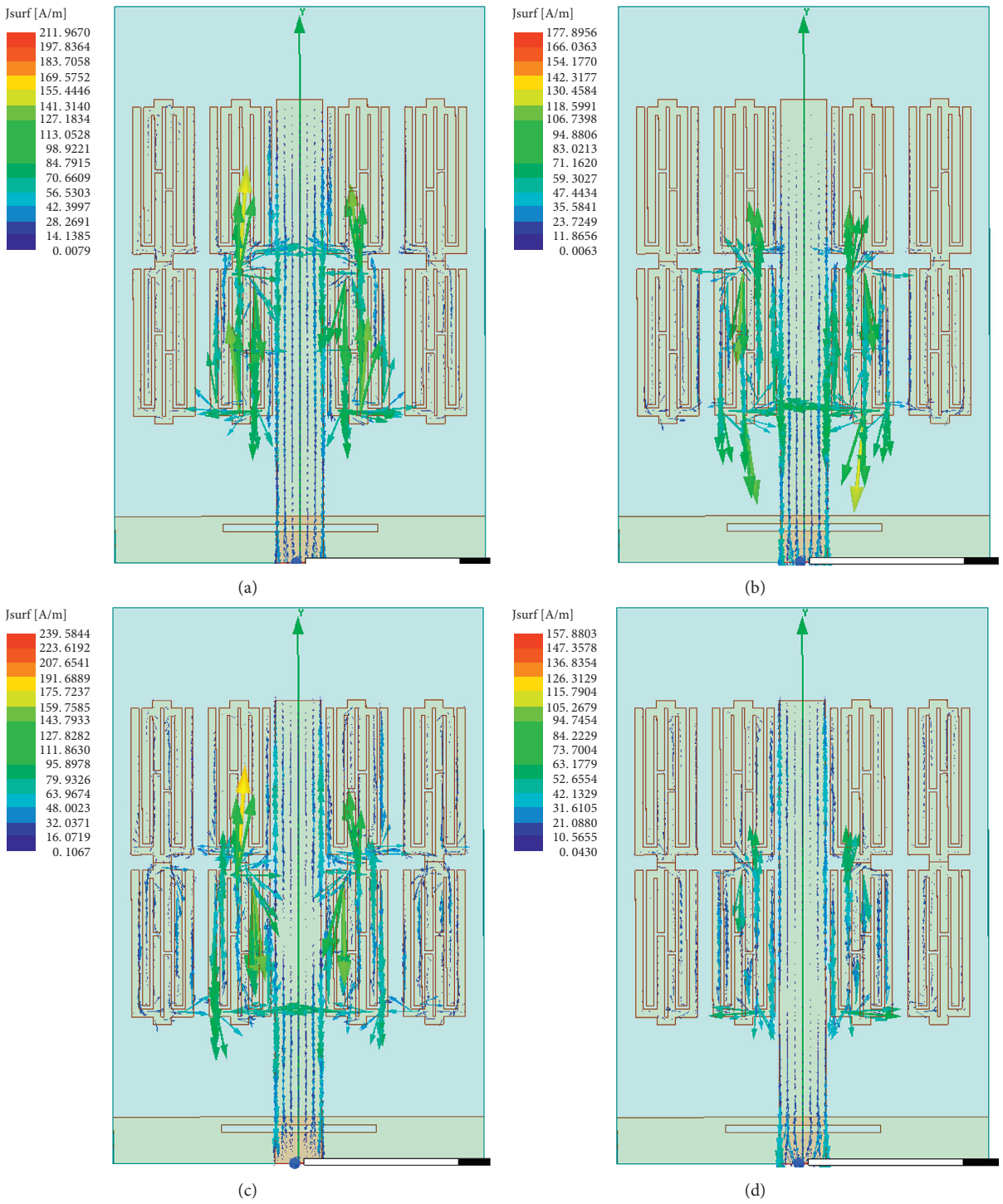

Figure 11: Current distribution at different frequencies of the proposed antenna: (a) 2.48 GHz, (b) 3.17 GHz, (c) 5.27 GHz, and (d) 7.22 GHz.

4. Conclusions

An LHM-inspired miniaturized quadband antenna is designed and analyzed in this paper. We first designed a novel LHM and then verified its double negative property through simulations and retrieved effective parameters. Then, this LHM is applied to surround a conventional monopole antenna. The proposed antenna is fabricated and discussed with simulations and measurements. A transmission line model for the proposed antenna is established to analyze the mechanism of miniaturization and multiband property. All the results indicate that near-field resonant

coupling between LHMs and the monopole brought miniaturization and multiband properties, and the proposed antenna is a good candidate for wireless communications.

Data Availability

The data used to support the findings of this study are included within the article.

Conflicts of Interest

The authors declare that they have no conflicts of interest.

Acknowledgments

This work is supported by the Natural Science Foundation of Jiangsu province of China (no. BK20190956).

References

[1] C. Wang, P. Xu, B. Li, and Z. H. Yan, "A compact multiband antenna for WLAN and WiMAX applications," *Microwave and Optical Technology Letters*, vol. 53, no. 9, pp. 2016–2018, 2011.

[2] J. Pei, A. G. Wang, S. Gao, and W. Leng, "Miniaturized triple-band Antenna with a defected ground plane for WLAN/WiMAX applications," *IEEE Antennas and Wireless Propagation Letters*, vol. 10, no. 4, pp. 298–301, 2011.

[3] A. K. Gautam, A. Bisht, and B. K. Kanaujia, "A wideband antenna with defected ground plane for WLAN/WiMAX applications," *AEU - International Journal of Electronics and Communications*, vol. 70, no. 3, pp. 354–358, 2016.

[4] A. Kunwar, A. K. Gautam, and K. Rambabu, "Design of a compact U-shaped slot triple band Antenna for WLAN/WiMAX applications," *AEUE - International Journal of Electronics and Communications*, vol. 71, 2016.

[5] S. M. Zhang, F. S. Zhang, W. Z. Li, T. Quan, and H. Y. Wu, "A compact UWB monopole antenna with wimax and WLAN band rejections," *Progress in Electromagnetics Research Letters*, vol. 31, pp. 159–168, 2012.

[6] A. K. Gautam, L. Kumar, B. K. Kanaujia, and K. Rambabu, "Design of compact F-shaped slot triple-band Antenna for WLAN/WiMAX applications," *IEEE Transactions on Antennas and Propagation*, vol. 64, no. 3, pp. 1101–1105, 2016.

[7] A. R. Jalali, J. Ahamdi-Shokouh, and S. R. Emadian, "Compact multiband monopole antenna for UMTS, WiMAX, and WLAN applications," *Microwave and Optical Technology Letters*, vol. 58, no. 4, pp. 844–847, 2016.

[8] A. D. Tadesse, O. P. Acharya, and S. Sahu, "Application of metamaterials for performance enhancement of planar antennas: a review," *International Journal of RF and Microwave Computer-Aided Engineering*, vol. 30, no. 5, p. e22154, n/a, 2020.

[9] C. Elavarasi and T. Shanmuganantham, "SRR loaded CPW-fed multiple band rose flower-shaped fractal antenna," *Microwave and Optical Technology Letters*, vol. 59, no. 7, pp. 1720–1724, 2017.

[10] R. Rajkumar and K. U. Kiran, "A metamaterial inspired compact open split ring resonator antenna for multiband operation," *Wireless Personal Communications*, vol. 97, pp. 1–15, 2017.

[11] R. S. Daniel, R. Pandeeswari, and S. Raghavan, "Design and analysis of metamaterial inspired open complementary split ring resonators for multiband operation," *Progress In Electromagnetics Research C*, vol. 78, pp. 173–182, 2017.

[12] S. Imaculate Rosaline and S. Raghavan, "Metamaterial inspired monopole antenna for WLAN/WiMAX applications," *Microwave and Optical Technology Letters*, vol. 58, no. 4, pp. 936–939, 2016.

[13] R. K. Saraswat and M. Kumar, "Miniaturized slotted ground UWB antenna loaded with metamaterial for WLAN and WiMAX applications," *Progress In Electromagnetics Research B*, vol. 65, pp. 65–80, 2016.

[14] G. Liu, Y. Liu, and S. Gong, "Compact tri-band wide-slot monopole antenna with dual-ring resonator for WLAN/WiMAX applications," *Microwave and Optical Technology Letters*, vol. 58, no. 5, pp. 1097–1101, 2016.

[15] A. Pirooj, M. Naser-Moghadasi, and F. B. Zarrabi, "Design of compact slot antenna based on split ring resonator for 2.45/5 GHz WLAN applications with circular polarization," *Microwave and Optical Technology Letters*, vol. 58, no. 1, pp. 12–16, 2016.

[16] T. Dong, X. Zhu, M. Li et al., "Design of electrically small Hilbert fractal NFRP magnetic monopole antennas," *Journal of Electromagnetic Waves and Applications*, vol. 33, no. 4, pp. 454–464, 2019.

[17] Z. Wu, M. C. Tang, M. Li, and R. W. Ziolkowski, "Ultra-low-profile, electrically small, pattern-reconfigurable metamaterial-inspired huygens dipole antenna," *IEEE Trans. Antennas Propag*, vol. 68, pp. 1238–1248, 2019.

[18] M. C. Tang and R. W. Ziolkowski, "Electrically small metamaterial-inspired antennas with active near field resonant parasitic elements: from theory to practice," in *Proceedings of the 2017 11th European Conference on Antennas and Propagation (EUCAP)*, pp. 1559–1563, IEEE, Paris, France, March 2017.

[19] S. Li, A. Elsherbeni, Z. Ding, and Y. Mao, "A metamaterial inspired compact miniaturized triple-band near field resonant parasitic antenna for WLAN/WiMAX applications," *Applied Computational Electromagnetics Society Journal*, vol. 35, no. 12, pp. 1539–1547, 2020.

[20] X. Chen, T. M. Grzegorczyk, B. I. Wu, J. Pacheco, and J. A. Kong, "Robust method to retrieve the constitutive effective parameters of metamaterials," *Physical review. E, Statistical, nonlinear, and soft matter physics*, vol. 70, no. 1, pp. 016608–016811, 2004.